Focusing of inertial waves by a vertically annular forcing

Jie Liu, Martin Oberlack, Yongqi Wang, Alexandre Delache, Fabien S Godeferd

Accepted to Phys. Fluids 10.1063/5.0099774

Focusing of inertial waves by a vertically annular forcing

J. Liu (刘杰),[1] M. Oberlack,[1] Y. Wang,[1] A. Delache,[2,3] and F. S. Godeferd[2]
[1)] *Chair of Fluid Dynamics, TU Darmstadt, Otto-Berndt-Str. 2, 64287 Darmstadt, Germany*
[2)] *Université de Lyon, École Centrale de Lyon, CNRS, Université Claude Bernard Lyon 1, INSA Lyon, LMFA, UMR5509, 69130 Ecully, France*
[3)] *Université Jean Monnet, 42100, Saint-Étienne, France.*

(*Electronic mail: oberlack@fdy.tu-darmstadt.de)

(Dated: 27 July 2022)

A theory of inertial wave focusing generated by a vertically oscillating slender torus immersed in a uniformly rotating fluid is presented. The analytical solution of the velocity field shows that, under an axisymmetric annular forcing in inviscid rotating fluid, the wave rays form a double cone symmetric about the plane on which the torus is located. At the two vertices of the double cone, the waves are in a shock-like manner focused causing localized surges of energy. After focusing, the waves continue their propagation and form a new inverted cone with the same cone angle, such that both cones are symmetric about the focal point. These results are in good agreement with the experimental and numerical study by M. Duran-Matute *et al.* [Phys. Rev. E 87, 041001(R) (2013)]. When friction effects occur, the wave pattern changes substantially and the wave away from the focal point is significantly attenuated so that the symmetry about the focal point is broken. As a consequence, the wave beam widens and the focusing effect becomes weaker with increasing Ekman number (*Ek*), which indicates the ratio of the viscous force to the Coriolis force. Furthermore, for the same *Ek*, the focusing effect tends to disappear when the forcing frequency is close to zero or twice the angular velocity of rotating flow. For forcing frequency close to the angular velocity of rotating fluid, the amplitude of the vertical velocity at the focal point reaches its maximum, which corresponds to a wave propagation angle of 60 degrees.

I. INTRODUCTION

Inertial waves can be generated in rotating flows as a result of the restoring action of the Coriolis force[1]. Purely inertial waves are relevant to industrial systems, such as fuel tanks in spacecraft or rotating turbines[2]. Clearly, one expects the presence of inertial waves in power-producing turbines, due to their size and their not too large rotation rates, unlike propulsion turbines with rotation rates much too large for inertial waves to have time to be present, even if there are no other disturbing phenomena (complex geometry, shocks, etc). Inertial waves are also of fundamental interest in geo- and astrophysical flows, for instance, in liquid planet cores[3], in the deep ocean or in the equatorial atmosphere[4]; in these cases they are often coupled with internal waves duo to density stratification effects[5]. A review of the known theories and properties of inertial and internal waves shows that they have great similarities in terms of physical phenomenon and mathematical treatment[6,7]. Both waves can be investigated individually but the results can be adopted almost identically. For instance, the propagation direction of their energy is determined only by the ratio between the wave frequency and the rotation rate of the fluid or the buoyancy frequency. As a consequence, their group and phase velocities are perpendicular to each other. Since only the orientation of the wave propagation is prescribed by the dispersion relation, the characteristics of the wave (wavelength and wave beam width) are independent of its frequency and are governed by boundary conditions, viscous dissipation[8,9] and eventually nonlinearities[10,11]. These properties lead to a wide variety of wave structures and wave phenomena. An important phenomenon concerns the conversion of wave energy into turbulent energy[12], which can be triggered by several mechanisms. In this paper, we are particularly interested in the wave focusing mechanism because it concentrates the wave energy in a small region of space and facilitates the conversion into turbulent energy. Triggering mixing at the focal point could be a way for new industrial processes in the chemical industry, or to make new materials or particles in suspension that cancel out the effect of gravity. In the case of geophysical flows, inertial waves may concentrate energy by focusing it in a particular region and possibly cascade energy locally into dissipative scales by nonlinear mechanisms. However, this is all speculative. Clarifying this issue requires further research. The aim of this article is to characterize this focusing of wave energies as a function of wave properties (frequency, phase shift and amplitude) and viscous properties of the fluid.

The focusing of conical waves was first noticed by Appleby and Crighton for the internal waves generated by an oscillating sphere in an inviscid stratified fluid[13]. The wave rays form a biconical structure on which the wave amplitude was singular, a phenomenon called caustic or focusing singularity. Simakov remarked that only the critical circles at which the wave rays are tangent to the sphere play a role in the formation of these singularities[14]. He replaced the sphere by a distribution of monopoles of a horizontal circle, and still observed focusing singularities. Then, he extended his conclusions to distributions of monopoles on curves and surfaces[15]. Independently, Tilgner considered the inertial waves generated by monopoles of oscillating strength distributed on disks and rings in a rotating fluid of low viscosity[16]. Wave beams formed along the rays, replacing the inviscid singularities there. Focusing took place at the points of convergence of the rays but went unnoticed. The same can be said for the vertical oscillations of a horizontal disk in a stratified fluid of low viscosity, considered by Bardakov *et al.*[17]. The next step came from Bühler and Muller[12], who looked at the horizontal oscillations of a stratified fluid over ring-shaped bottom topography of Gaussian cross-section. The nonzero size of the section allowed the

Accepted to Phys. Fluids 10.1063/5.0099774

determination of the amplification rate of the waves owing to focusing, namely the ratio between the wave amplitudes at the focus and at the topography. This rate was found proportional to the square root of the aspect ratio between the radius of the torus and the radius of the tube. Non-axisymmetric rings were also investigated, either elliptic[12] or horseshoe-shaped[18]. For inertial waves, Le Dizès and Le Bars considered the libration of a circular disk and also observed focusing, associated with the waves emanating from the rim of the disk, which forms an effective Dirac ring source[19,20]. They proposed a description of the focal region by matched asymptotic expansions, obtaining both waves and a mean flow generated by the nonlinear interaction of the waves with themselves.

The first experimental and numerical demonstration of conical wave focusing was given by Duran-Matute *et al.*[21], using the vertical oscillations of a horizontal torus in a uniformly rotating fluid. Ermanyuk *et al.* and Shmakova & Flór performed the same in a stratified fluid[11,22], using the horizontal oscillations of a horizontal torus. They paid more attention to the linear and nonlinear regimes, respectively. The cross-section of the torus was small enough for the wave beams to be dominated by viscosity, having unimodal profiles with a single peak of the amplitude at their centre, corresponding to the wave ray through the centre of the cross-section. Shmakova *et al.* used a bigger torus to reach the parameter range where the wave profile is bimodal, with two peaks of the amplitude at the sides, corresponding to the wave rays tangential to the cross-section on either side[23].

Ermanyuk *et al.* also proposed a quasi-two-dimensional theory of focusing, considering the interference of the two cross-sections in the same azimuthal plane and driving the result by the inverse square root of the horizontal distance to the axis, in order to conserve the wave energy in the cylindrical geometry[22]. The theory failed close to the axis, hence could not be used to calculate the waves in the focal region. Voisin[24] proposed a full three-dimensional theory for large aspect ratio, corrected later by Shmakova *et al.*[23] and yielding reasonable agreement with their experiments.

Inertial waves can also be generated by global forcing in the form of precession and libration of rotating systems[25,26]. Particularly, in a precession-driven flow in a cylindrical cavity, the wave beams arise locally in the corners of the finite cylinder, similar to the effect produced by an annular forcing. Although these wave beams are non-axisymmetric due to the non-axisymmetric forcing, focusing and amplification phenomena have been observed as well and an impact on the dynamics of the flow has been suspected[27,28].

The aim of the present investigation is to develop a theory for the "shock-like" focusing of inertial waves observed by Duran-Matute *et al.*[21]. A schematic drawing is shown in Fig. 1. Different wave generators can be used. In contrast to the models established by Machicoane *et al.*[29], Voisin[24] and Shmakova *et al.*[23], in which the wave generator is presented as a source of mass releasing fluid, we currently consider the vertically vibrating torus as an annular line force. The corresponding inertial wave equations are first derived from the linearized Navier-Stokes equations including the force from the torus exerted on the fluid. With the help of the Fourier transform

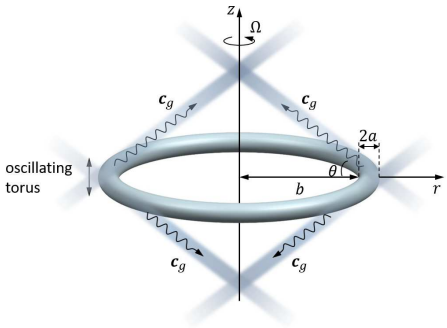

FIG. 1. Schematic drawing of the oscillating torus and the focusing effect of the resulting inertial waves, where a is the radius of the tube and b the major radius of the torus with $a \ll b$, Ω is the constant angular velocity of the rotating flow. c_g denotes the group velocity, at which the wave energy propagates, and θ is the propagation angle.

in cylindrical coordinate system, the particular solutions of the velocity field are obtained for the inviscid and the viscous case, respectively. The analytical results in the inviscid case describe the generation, propagation and focusing of inertial waves, which show good agreement with the experimental and numerical results of Duran-Matute *et al.*[21]. The annular forcing generates inertial waves that propagate along a double cone that is symmetrical about the torus and has two focal points, where inertial waves focus around the apex of the cone. At the focal zone, the amplitude of the waves may no longer be small, i.e. non-linearity may become to be important in, and a net transfer of energy between two waves may occur. In turn, a patch of turbulence may develop locally. Additionally, a theoretical model for a viscous fluid has been developed to study the effect of viscous attenuation on the focusing phenomenon. Our analysis shows that as the Ekman number increases, the wave beam becomes wider and and the focusing effect becomes weaker. For the non-dimensional oscillation frequency σ, i.e. the ratio between the oscillation frequency of the torus and the angular velocity of the rotating fluid, close to 0 and 2, the focusing effect tends to disappear, while the maximum appears for σ close to 1, which corresponds to a wave angle of $\theta = 60°$. A similar focusing effect was discussed for internal waves in stratified fluid by Shmakova & Flór[11], but has never been analysed in detail for inertial waves.

In this article, the linear theory of inertial waves focusing in a rotating fluid of uniform density will be first presented in Sec. II. Then, the predictions of this theory on the characteristics of the focusing zone in terms of viscous spreading and maximum amplification are shown in Sec. III and various results aided by MATLAB. Finally, conclusions are drawn in Sec. IV.

Accepted to Phys. Fluids 10.1063/5.0099774

II. LINEAR ANALYSIS OF FOCUSING WAVES

A. Wave-like equations

We consider a uniformly rotating fluid with angular velocity $\boldsymbol{\Omega}$, density ρ and kinematic viscosity ν. The dynamics of the flow can be described by the Navier-Stokes equations including the Coriolis force[1]. For low-amplitude disturbances, the departures of pressure p and velocity $\boldsymbol{u}$ from the undisturbed rotating flow are governed by the linearized equations of motion

$$\frac{\partial \boldsymbol{u}}{\partial t} + 2\boldsymbol{\Omega}\times\boldsymbol{u} = -\frac{1}{\rho}\nabla p + \nu\nabla^2\boldsymbol{u} + \boldsymbol{f}, \tag{1}$$

$$\nabla\cdot\boldsymbol{u} = 0. \tag{2}$$

Here p represents the reduced pressure, which includes the hydrodynamic pressure and the centrifugal force. The annular forcing is modelled as a body force $\boldsymbol{f}$ per unit mass. Further, let L, Ω^{-1}, U characterize the typical length, time and relative fluid velocity to the rotating flow. The replacement of the variables $\boldsymbol{x}$, t, $\boldsymbol{u}$, $\boldsymbol{\Omega}$, p, $\boldsymbol{f}$ by their scaled counterparts $L\boldsymbol{x}$, $\Omega^{-1}t$, $U\boldsymbol{u}$, $\Omega\boldsymbol{n}$, $\rho\Omega ULp$, $\Omega U\boldsymbol{f}$ allows the reduction of the linearized equation system to a dimensionless form

$$\frac{\partial \boldsymbol{u}}{\partial t} + 2\boldsymbol{n}\times\boldsymbol{u} = -\nabla p + Ek\nabla^2\boldsymbol{u} + \boldsymbol{f}, \tag{3}$$

$$\nabla\cdot\boldsymbol{u} = 0, \tag{4}$$

where $\boldsymbol{n}$ is a unit vector indicating the direction of the rotation axis. The Ekman number $Ek = \frac{\nu}{\Omega L^2}$ is a gross measure of the viscous force compared to the Coriolis force.
Applying the operator $(\frac{\partial}{\partial t}\nabla\times\nabla\times)$ to Eq. (3) and taking the continuity condition in Eq. (4) into account lead to a single wave-like equation for the velocity $\boldsymbol{u}$ in the form

$$\begin{aligned}&\left(\frac{\partial}{\partial t} - Ek\nabla^2\right)^2\nabla^2\boldsymbol{u} + (2\boldsymbol{n}\cdot\nabla)^2\boldsymbol{u}\\ &= -2(\boldsymbol{n}\cdot\nabla)(\nabla\times\boldsymbol{f}) - \left(\frac{\partial}{\partial t} - Ek\nabla^2\right)[\nabla\times(\nabla\times\boldsymbol{f})].\end{aligned} \tag{5}$$

Analogously, we can also eliminate the velocity $\boldsymbol{u}$ by applying the operator $(\frac{\partial^2}{\partial t^2}\nabla\cdot)$ to Eq. (3) and reducing the result with the continuity equation (4). This yields a single wave-like equation for the pressure, i.e.

$$\begin{aligned}&\left(\frac{\partial}{\partial t} - Ek\nabla^2\right)^2\nabla^2 p + (2\boldsymbol{n}\cdot\nabla)^2 p = 4\boldsymbol{n}\cdot(\boldsymbol{n}\cdot\nabla)\boldsymbol{f}\\ &+ 2\boldsymbol{n}\cdot\left(\frac{\partial}{\partial t} - Ek\nabla^2\right)(\nabla\times\boldsymbol{f}) + \left(\frac{\partial}{\partial t} - Ek\nabla^2\right)^2(\nabla\cdot\boldsymbol{f}).\end{aligned} \tag{6}$$

The homogeneous parts of the wave-like equations (5) and (6) support plane wave solutions which are known as inertial waves[1]. The focusing phenomenon caused by the forcing $\boldsymbol{f}$ is contained in the particular solutions, which is the key topic of the present analysis. For this, we consider an infinite fluid domain and mainly investigate the properties of the forced inertial waves emitted from a monochromatic oscillating torus, as shown in Fig. 1.

B. Modeling the forcing condition

It is assumed that the oscillation of the torus is monochromatic, axisymmetric and only in the vertical direction. In addition, the radius of the tube a is much smaller than the major radius of the torus b, so that the force of the torus to the fluid can be considered as a line force. We choose b as the characteristic length L for nondimensionalization of the system, then the Ekman number is represented as

$$Ek = \frac{\nu}{\Omega b^2}. \tag{7}$$

We define the cylindrical coordinate system $(\vec{e}_r, \vec{e}_\varphi, \vec{e}_z)$ with $\vec{e}_z$ parallel to the axis of the rotation. The forcing $\boldsymbol{f}$ has only one component in z-direction, i.e. $\boldsymbol{f} = (0, 0, f_z)$, which can be described using the Dirac function as follows

$$f_z(r,\varphi,z,t) = \Lambda(\varphi)\delta(r-1)\delta(z)e^{-i\sigma t}. \tag{8}$$

Here σ is the ratio between the oscillation frequency of the torus and the rotation rate Ω of the fluid. $\Lambda(\varphi)$ denotes a line density of the force along the torus, which may be expanded in a Fourier series as

$$\Lambda(\varphi) = \sum_{m=-\infty}^{+\infty}\Lambda_m e^{im\varphi}, \tag{9}$$

where m denotes the azimuthal wave number and Λ_m the corresponding forcing amplitude (or weight). The superposition of appropriate combinations of m and Λ_m can approximate an arbitrary function and be used to describe any form of distribution of the force density along the torus, such as non-axisymmetric forcing on an elastic ring. For the rigid torus used in the study by Duran-Matute *et al.*[21], the force distribution is axisymmetric and only the case $m = 0$ needs to be considered.
In the following, we shall investigate the distribution of the velocity field exclusively under the forcing condition described in Eq. (8) by solving the wave-like equations (5) and (6) for an inviscid and viscous fluid, respectively.

C. Inviscid case

A convenient starting point to analyse the properties of the inertial waves excited by an annular force is firstly to ignore the effect of viscosity, i.e. $Ek = 0$. The left sides of the equations (5) and (6) have a comparable structure. Their difference is only in the inhomogeneous terms. Especially, in the Cartesian coordinate system, the analysis of these two equations is also similar. For this case, we can obtain both velocity $\boldsymbol{u}$ and pressure p directly from their corresponding wave-like equations (5) and (6). Alternatively, we can also solve one of the wave-like equations firstly and then bring the result back to the momentum equation (3) to solve for the other variable. In the context of the annular forcing described in (8), the cylindrical coordinate system is the most convenient choice. However, in the cylindrical coordinate system the components of the vector

Accepted to Phys. Fluids 10.1063/5.0099774

equation (5) are coupled to each other, the solving this vector equation is much more complex than the scalar equation (6). For this reason, we prefer to start by solving the wave-like equation (6) for the pressure p, and then bring its solution back to the momentum equation (3) to analyse the velocity field instead of solving the wave-like equation (5) directly.
Under the forcing condition (8) and the assumption of an inviscid fluid, the wave-like equation (6) yields

$$\frac{\partial^2}{\partial t^2}\nabla^2 p + 4\frac{\partial^2 p}{\partial z^2} = \left(4-\sigma^2\right)\delta(r-1)\delta'(z)\sum_{m=-\infty}^{+\infty}\Lambda_m e^{i(m\varphi-\sigma t)}. \tag{10}$$

Generally, the homogeneous part of this equation supports plane wave solution[1] of the form

$$p = P(\boldsymbol{k})e^{i(\boldsymbol{k}\cdot\boldsymbol{x}-\sigma t)}, \tag{11}$$

where $\boldsymbol{x}$ describes the position and $\boldsymbol{k}$ the wave vector. Furthermore, the substitution of the expression (11) into the homogeneous part of (10) leads to the dispersion relation

$$\sigma^2 k^2 - 4k_z^2 = 0, \tag{12}$$

where k denotes the modulus of $\boldsymbol{k}$. In any azimuthal plane in cylindrical coordinate system, the wave vector can be described as $\boldsymbol{k} = (k_r, \varphi_k, k_z)$ and its modulus as $k = (k_r^2 + k_z^2)^{1/2}$. The relation (12) describes a wavenumber surface for frequency σ in the (k_r, k_z) plane in the shape of a St. Andrew's cross. In addition, the group velocity $\boldsymbol{c}_g$, at which the wave energy propagates, can be derived from (12) according to the definition

$$\boldsymbol{c}_g = \left(\frac{\partial\sigma}{\partial k_r}, \frac{\partial\sigma}{\partial k_z}\right) = \mathrm{sign}(k_z)\frac{2k_r}{k^3}(-k_z, k_r). \tag{13}$$

As a consequence, in any azimuthal plane the group velocity $\boldsymbol{c}_g$ is perpendicular to the wave vector $\boldsymbol{k} = (k_r, k_z)$ and forms another axisymmetric St. Andrew's cross in the physical plane by an angle

$$\theta = \cos^{-1}(\sigma/2) \tag{14}$$

with respect to the horizontal, as shown in Fig. 1.
To analyse the inhomogeneous solution of the wave-like equation (6), we introduce the Fourier transform of an arbitrary function $\chi(r,\varphi,z)$ and its inverse in the cylindrical coordinate system defined as

$$\begin{aligned}\hat{\chi}(k_r,\varphi_k,k_z) = &\int_{-\infty}^{\infty}\int_0^{2\pi}\int_0^{\infty}\chi(r,\varphi,z)\\ &\times e^{-i[k_r r\cos(\varphi-\varphi_k)+k_z z]}r\,dr\,d\varphi\,dz,\end{aligned} \tag{15}$$

$$\begin{aligned}\chi(r,\varphi,z) = &\frac{1}{(2\pi)^3}\int_{-\infty}^{\infty}\int_0^{2\pi}\int_0^{\infty}\hat{\chi}(k_r,\varphi_k,k_z)\\ &\times e^{i[k_r r\cos(\varphi-\varphi_k)+k_z z]}k_r\,dk_r\,d\varphi_k\,dk_z.\end{aligned} \tag{16}$$

According to (15), the transformation of the wave-like equation (10) for the pressure $p(r,\varphi,z,t)$ into Fourier space results in the following equation

$$\begin{aligned}&k^2\frac{\partial^2}{\partial t^2}\hat{p} + 4k_z^2\hat{p}\\ &= -2\pi\left(4-\sigma^2\right)k_z\sum_{m=-\infty}^{+\infty}i^{1-m}\Lambda_m J_m(k_r)e^{i(m\varphi_k-\sigma t)},\end{aligned} \tag{17}$$

and its solution for the inhomogeneous part reads as follows

$$\hat{p} = \frac{2\pi\left(4-\sigma^2\right)k_z}{\sigma^2k^2 - 4k_z^2}\sum_{m=-\infty}^{+\infty}i^{1-m}\Lambda_m J_m(k_r)e^{i(m\varphi_k-\sigma t)}. \tag{18}$$

where $J_m(k_r)$ is the Bessel function of the first kind.
Replacing k^2 with $k_r^2 + k_z^2$ and applying the inverse Fourier transform in the cylindrical coordinate system, as defined in (16), we obtain the solution of the pressure p in physical space

$$\begin{aligned}p = &-\frac{i(4-\sigma^2)}{2\pi}\sum_{m=-\infty}^{+\infty}\Lambda_m e^{i(m\varphi-\sigma t)}\\ &\times\int_{-\infty}^{\infty}\int_0^{\infty}\frac{k_z J_m(k_r)J_m(k_r r)}{(4-\sigma^2)k_z^2 - \sigma^2k_r^2}e^{ik_z z}k_r\,dk_r\,dk_z,\end{aligned} \tag{19}$$

Depending on whether the forcing frequency exceeds twice the rotational frequency, i.e. $|\sigma| < 2$ or $|\sigma| > 2$, two very different modes of responses are distinguished in the linear problem.
For the case $|\sigma| < 2$, the integral over k_z in Eq. (19) is mathematically ambiguous, which corresponds to a genuine physical ambiguity. The energy of the forced waves might be moving radially inwards towards the source region, having been generated at infinity. Therefore, the mathematical problem fails to represent completely the physical problem of finding the waves generated by the source itself. The physical issues discussed in this study must be subject to the radiation conditions[5], that is, no wave energy is being generated at infinity. This requirement is met by replacing σ by $\sigma + i\epsilon$ with $\epsilon > 0$. Here, ϵ is small and will be ultimately allowed to tend to zero. Applying the residue theorem[30], the integral in (19) with respect to k_z for the case $|\sigma| < 2$ can be evaluated unambiguously along the real k_z-axis, which leads to the result

$$\begin{aligned}p = &\,\mathrm{sign}(z)\sum_{m=-\infty}^{+\infty}\frac{\Lambda_m}{2}e^{i(m\varphi-\sigma t)}\\ &\times\int_0^{\infty}k_r J_m(k_r)J_m(rk_r)e^{i\alpha|z|k_r}\,dk_r,\end{aligned} \tag{20}$$

where

$$\alpha = \sqrt{\frac{\sigma^2}{4-\sigma^2}}. \tag{21}$$

For the case of relatively rapidly oscillating forcing. i.e. $|\sigma| > 2$, the integral in (19) with respect to k_z yields[31]

$$\begin{aligned}p = &\,\mathrm{sign}(z)\sum_{m=-\infty}^{+\infty}\frac{\Lambda_m}{2}e^{i(m\varphi-\sigma t)}\\ &\times\int_0^{\infty}k_r J_m(k_r)J_m(rk_r)e^{-\gamma|z|k_r}\,dk_r\end{aligned} \tag{22}$$

Accepted to Phys. Fluids 10.1063/5.0099774

with $\gamma = \sqrt{\frac{\sigma^2}{\sigma^2-4}}$.

The solutions (20) and (22) show mathematically that inertial waves can only be excited when the forcing frequency is smaller than twice the angular velocity of basic rotation, i.e. $|\sigma| < 2$. For $|\sigma| > 2$ there are no wave phenomena observed. However, the method breaks down if $|\sigma| = 2$. For this case, the inhomogeneous part of the wave-like equation (10) vanishes, the forcing effect disappears and the boundary conditions dominate the wave phenomenon. This must be treated as a limiting case and will not be discussed in this investigation. Physically, inertial waves are related to inertia and are based on the response of fluid parcels to the Coriolis force in a rotating system, so that the inertial timescale limits the frequency at which they can be pushed by it. Furthermore, inertial waves are associated to circling motion of the fluid particles in planes that form an angle with the rotation axis[32]. These special mechanisms make it impossible to form and propagate inertial waves with frequencies higher than twice the rotating frequency of the fluid, and thus there is no focusing of the waves.

In the following analysis, we will restrict the non-dimensional frequency to $|\sigma| < 2$ and further analyze the distribution of the velocity field. The associated velocity components in the radial direction u_r, in the azimuthal direction u_φ and in the vertical direction u_z can be determined directly by substituting the solution of the pressure (20) into the momentum equation (3). As a result we obtain the following solutions for the velocity components (details in appendix A):

$$u_r = -\operatorname{sign}(z)\frac{i\alpha^2}{2\sigma^2}\sum_{m=-\infty}^{+\infty}\Lambda_m e^{i(m\varphi-\sigma t)}\int_0^\infty e^{i\alpha|z|k_r}k_r^2 J_m(k_r) \times\left[\left(1-\frac{\sigma}{2}\right)J_{m-1}(rk_r)+\left(1+\frac{\sigma}{2}\right)J_{m+1}(rk_r)\right]dk_r, \tag{23}$$

$$u_\varphi = \operatorname{sign}(z)\frac{\alpha^2}{2\sigma^2}\sum_{m=-\infty}^{+\infty}\Lambda_m e^{i(m\varphi-\sigma t)}\int_0^\infty e^{i\alpha|z|k_r}k_r^2 J_m(k_r) \times\left[\left(1-\frac{\sigma}{2}\right)J_{m-1}(rk_r)-\left(1+\frac{\sigma}{2}\right)J_{m+1}(rk_r)\right]dk_r, \tag{24}$$

$$u_z = \frac{\alpha}{2\sigma}\sum_{m=-\infty}^{+\infty}\Lambda_m e^{i(m\varphi-\sigma t)} \times\int_0^\infty k_r^2 J_m(k_r)J_m(k_r r)e^{i|z|\alpha k_r}dk_r. \tag{25}$$

In the above solutions of the velocity components, we have not been able to further calculate the integrals with respect to k_r analytically. To proceed further, we evaluated the integrals numerically and plotted the solutions. To compare our analytical results with the experimental and numerical study by Duran-Matute *et al.*[21], we focus our analysis on the axisymmetric case, i.e. $m = 0$.

Fig. 2 shows the isosurface of the vertical velocity component u_z according to the solution (25) for the case $\sigma = \sqrt{2}$. The cone-shaped wave beam of inertial waves excited by the oscillating torus can be clearly observed. The distribution of the velocity field is axisymmetric about the z-axis due to the axisymmetric forcing. Therefore, we only need to observe the wave beam in one quadrant for the following analysis.

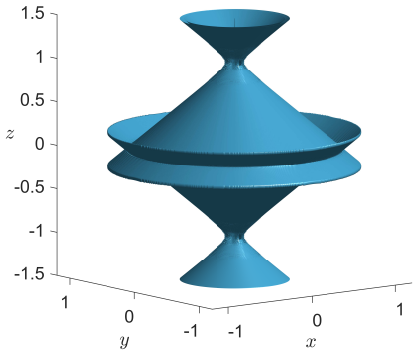

FIG. 2. Cone of inertial waves excited by the oscillating torus depicted by the isosurface of the amplitude of $|u_z| = 12$ according to the analytical solution (25) for $m = 0$, $\Lambda_0 = 0.01$ and $\sigma = \sqrt{2}$.

Fig. 3 shows the distribution of the velocity components according to the solutions in (23), (24) and (25) only in the vertical plane (r,z) for $\sigma = 1$ and $\sigma = \sqrt{2}$, respectively. To avoid divergence at the focal point (see the discussion below the Eq. 26), a cut-off at $\bar{k}_r = 300$ was introduced. From Fig. 3, we can intuitively see that all three velocity components are mainly distributed in the wave beam around an angle of $\theta = 45°$ to the horizontal for $\sigma = \sqrt{2}$ and at $\theta = 60°$ for $\sigma = 1$, which represents the direction of energy propagation of the inertial waves. This result agrees exactly with the dispersion relation determined by Eq. (14). Due to the axisymmetric propagation direction, the waves are focused in a small region on the z-axis. After focusing, the rays form a new inverted cone-shaped wave beam with the same angle to the horizontal.

According to the dispersion relation determined by the frequency σ, we can expect that the focusing of the waves occurs at $r = 0, z = 1/\alpha$ with α defined in equation (21). At this point, the velocity components u_r and u_φ are both zero according to (23) and (24), and the vertical velocity (25) reduces to

$$u_z = \frac{\Lambda_0\alpha}{2\sigma}e^{-i\sigma t}\int_0^\infty k_r^2 J_0(k_r)e^{ik_r}dk_r. \tag{26}$$

This integral may be written in terms of hypergeometric functions. However, it diverges if there are no other conditions to restrict the upper limit of k_r. A reason for this infinity is that in the region around the focal point, the assumption of small amplitudes is no longer suitable, non-linearities may become important and an energy transfer between the waves can take place. The other reason for the appearance of this singularity is closely related to the neglect of viscosity. In the following, we will analyze the effect of viscosity on the focusing phenomenon of inertial waves stimulated by an axisymmetric

Accepted to Phys. Fluids 10.1063/5.0099774

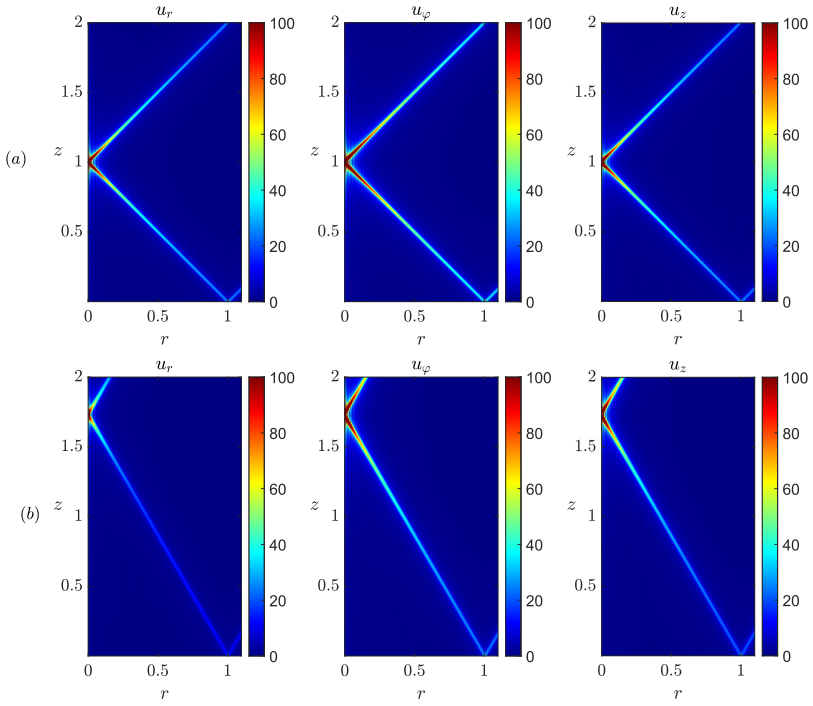

FIG. 3. Amplitude of the velocity components u_r, u_φ and u_z in the vertical plane for $m = 0$ with a cut-off at $\bar{k}_r = 300$ for (a) $\sigma = \sqrt{2}$ $(\theta = 45°)$ and (b) $\sigma = 1$ $(\theta = 60°)$.

forcing.

D. Viscous case

The viscous spreading of the wave beam results from the combination of the energy propagation in the direction of the group velocity and its diffusion in the lateral direction[29,33]. Due to the similar distributions of all velocity components observed from the results of the previous part, we will analyze the effect of viscosity on the energy propagation and the phenomenon of inertial wave focusing in a viscous fluid by only studying the vertical velocity component u_z under an axisymmetric forcing.

Considering the forcing condition (8) with $m = 0$, the wave-like equation for the pressure (6) in a viscous fluid is given by

$$\left(\frac{\partial}{\partial t} - Ek\nabla^2\right)^2 \nabla^2 p + 4\frac{\partial^2 p}{\partial z^2} = \Lambda_0 \left[4 - \left(\sigma - iEk\nabla^2\right)^2\right] \delta(r-1)\delta'(z) e^{-i\sigma t}. \tag{27}$$

For the analysis below we need to understand that the dispersion relation (12), which has been derived for the inviscid case, is also valid for the viscous case. This can be easily demonstrated by extending the solution in (11) to the following form

$$p = P(\boldsymbol{k}) e^{i(\boldsymbol{k}\cdot\boldsymbol{x} - \sigma t)} e^{-Ek|\boldsymbol{k}|^2 t}, \tag{28}$$

as introduced by Greenspan[1] in chapter 4. The substitution of (28) into the homogeneous part of (27) leads to the same dispersion relation as described in (12).

Analogous to the analysis in inviscid case, by using the Fourier transform in cylindrical coordinate system, we obtain the inhomogeneous solution for the pressure in Fourier space

$$\hat{p}(k_r, k_z, t) = i2\pi\Lambda_0 e^{-i\sigma t} \frac{\left[4 - \left(\sigma + iEk\,k^2\right)^2\right] k_z J_0(k_r)}{\left(\sigma + iEk\,k^2\right)^2 k^2 - 4k_z^2}. \tag{29}$$

Additionally, the transformation of the momentum equation (3) in z-direction into Fourier space results in the following scalar equation

$$\left(\frac{\partial}{\partial t} + Ek\,k^2\right) \hat{u}_z = -ik_z \hat{p} + \hat{f}_z, \tag{30}$$

where $\hat{f_z} = 2\pi\Lambda_0 J_0(k_r)e^{-i\sigma t}$. Substituting (29) into (30), the inhomogeneous solution of u_z in Fourier space follows as

$$\hat{u}_z = i2\pi\Lambda_0 e^{-i\sigma t}\frac{J_0(k_r)k_r^2\left(\sigma + iEk\,k^2\right)}{\left(\sigma + iEk\,k^2\right)^2 k^2 - 4k_z^2}. \tag{31}$$

According to the inverse Fourier transform in Eq. (16) and applying the residue theorem for the integral with respect to k_z, we eventually obtain the solution of u_z in physical space (details in appendix B)

$$u_z = e^{-i\sigma t}\frac{\Lambda_0}{2}\int_0^\infty k_r^3 J_0(k_r)J_0(rk_r)\frac{[\sigma(4-\sigma^2)f_1 + 4Ek\,k_r^2 f_2] + i[4Ek\,k_r^2 f_1 - \sigma(4-\sigma^2)f_2]}{\sigma(4-\sigma^2)^{3/2}(f_1^2+f_2^2)}e^{i|z|\alpha f_1}e^{-|z|\alpha f_2}dk_r, \tag{32}$$

where we recall $\alpha = \frac{\sigma}{\sqrt{4-\sigma^2}}$, and

$$f_{1,2} = \frac{k_r}{\sqrt{2}}\sqrt{\sqrt{\left[1-\frac{64Ek^2k_r^4}{\sigma^2(4-\sigma^2)^3}\right]^2 + \frac{1024Ek^2k_r^4}{\sigma^2(4-\sigma^2)^4}} \pm \left[1-\frac{64Ek^2k_r^4}{\sigma^2(4-\sigma^2)^3}\right]}. \tag{33}$$

III. CHARACTERISTIC OF THE FOCUSING ZONE

A. Viscous effect on the wave focusing

The result (32) is plotted in Fig. 4 for $\sigma = 1$ and the Ekman number Ek= 10^{-5}, 10^{-4} and 10^{-3}, respectively. Obviously, the solution (32) can describe the viscous spreading, i.e. in a viscous fluid. Since the oscillating torus with a dimensionless radius $r = 1$ is in the plane $z = 0$, see Sec. II B, the velocity distribution in this region around $z = 0$ and $r = 1$ describes the direct response of the fluid duo to the forcing. The wave beam becomes wider the further away it is from the oscillating source. This effect of viscous spreading was also observed in the laboratory experiment[33]. In addition, as the value of the Ekman number increases, the effect of viscous attenuation becomes stronger, which leads to a rapid dissipation of energy during the propagation. As a result, with increasing viscosity the focal zone becomes increasingly blurred and the amplitude of the waves is greatly reduced compared to the case in an inviscid fluid. The observed phenomenon, especially also the elongated axisymmetric structure near the focal point in figure 4(c), is strongly reminiscent of the Direct Numerical Simulation and experimental results by Duran-Matute *et al.*[21]. In fact, the value of the Ekman number used in Fig. 4(c), Ek= 10^{-3}, corresponds to a viscosity much larger than its molecular value. Therefore, this case can be interpreted as a phenomenon of the mean velocity in a turbulent case in which a large constant eddy viscosity was used instead of the molecular viscosity. Next, we will use the analytical solution to further qualitatively analyze the effect of viscosity on the focusing phenomenon of inertial waves.

In order to be able to analyze the viscous effect described in (32) more intuitively, we further simplify it by introducing the assumption of small Ekman number, i.e. $Ek \ll 1$. Using Taylor expansion and neglecting all terms with $O(Ek^2)$, f_1 and f_2 in (33) can be simplified to the following approximations

$$f_1 \approx k_r, \tag{34a}$$

$$f_2 \approx \frac{16Ek\,k_r^3}{\sigma(4-\sigma^2)^2}. \tag{34b}$$

Correspondingly, the solution of u_z in (32) can be simply expressed as

$$u_z \approx e^{-i\sigma t}\frac{\Lambda_0}{2}\int_0^\infty \frac{(4-\sigma^2)^2 - i4\sigma Ek\,k_r^2}{(4-\sigma^2)^{5/2}}k_r^2 J_0(k_r)J_0(rk_r) \times e^{i|z|\alpha k_r}e^{-|z|\alpha\beta k_r^3}dk_r. \tag{35}$$

Using Euler's formula and considering small-Ek assumption, this result can be further simplified to

$$u_z \approx e^{-i\sigma t}\int_0^{\bar{k}_r} Ae^{i(|z|\alpha k_r - \psi)}e^{-|z|\alpha\beta k_r^3}dk_r \tag{36}$$

with

$$A = \frac{\Lambda_0\alpha}{2\sigma}k_r^2 J_0(k_r)J_0(rk_r), \tag{37a}$$

$$\psi = \arctan\frac{4\sigma Ek\,k_r^2}{(4-\sigma^2)^2}, \tag{37b}$$

$$\beta = \frac{16Ek}{\sigma(4-\sigma^2)^2}. \tag{37c}$$

Here A denotes the amplitude as in the inviscid fluid, ψ represents the phase shift and β is a factor that describes the attenuation due to viscosity. It is to be noted that both ψ and β are affected not only by the viscosity but also by the forcing frequency. The larger ψ and β are, the wider is the wave beam and weaker is the focusing effect.

At the focal point, where $r = 0$ and $|z| = 1/\alpha$, the effect of viscous attenuation is actually dominated by the factor $e^{-\beta k_r^3}$, which decays rapidly as k_r increases. Fig. 5 shows, the exponential function $e^{-\beta k_r^3}$ converges to zero at a smaller wavenumber k_r with increasing value of Ek as well as $\sigma \to 0$ and $\sigma \to 2$.

Accepted to Phys. Fluids 10.1063/5.0099774

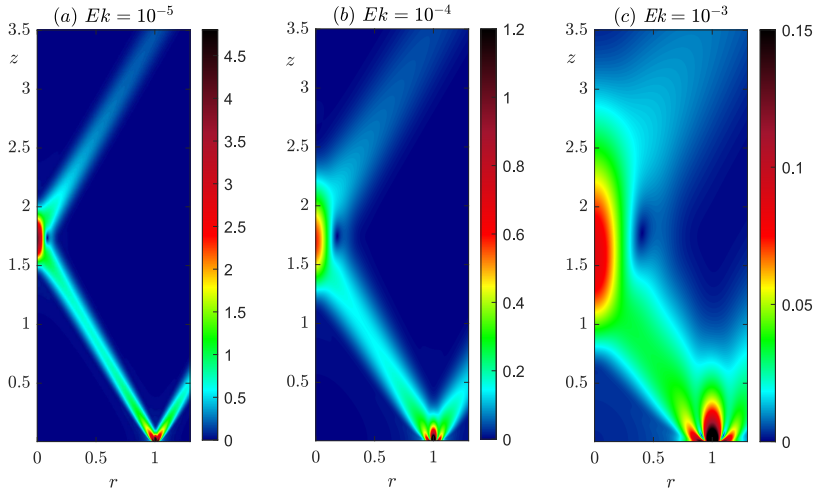

FIG. 4. Amplitude of the vertical velocity in the vertical plane for $\sigma = 1$ in a viscous fluid with the Ekman number (*a*) $Ek = 10^{-5}$, (*b*) $Ek = 10^{-4}$ and (*c*) $Ek = 10^{-3}$, respectively.

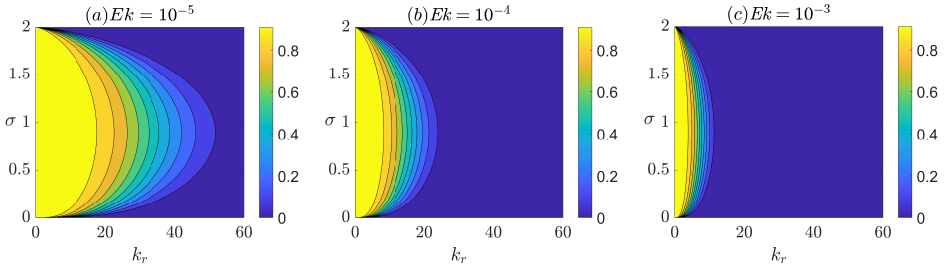

FIG. 5. Plot of the function $e^{-\beta k_r^3}$ with the change of σ and k_r for the Ekman number (*a*) $Ek = 10^{-5}$, (*b*) $Ek = 10^{-4}$ and (*c*) $Ek = 10^{-3}$, respectively.

For this we postulate the existence of a cutoff wavenumber $\bar{k}_r$ so that viscous attenuation eliminates all waves with the wavenumbers that are significantly greater than $\bar{k}_r$. In numerical evaluation, an attenuation factor e^{-c} can be predefined, where the constant c is used to control the precision of the integration result. As an example, the choice of $c = 10$ corresponds to an attenuation factor $e^{-c} \approx 4.5 \times 10^{-5}$, which may be sufficiently small for applications. The value of cutoff wavenumber $\bar{k}_r$ of the function $e^{-\beta k_r^3}$ corresponding to the chosen attenuation factor e^{-c} can be reasonably estimated by

$$\bar{k}_r = \left(\frac{c}{\beta}\right)^{1/3} = \left[\frac{c\sigma(4-\sigma^2)^2}{16Ek}\right]^{1/3}. \tag{38}$$

Eq. (38) shows that for the same non-dimensional forcing frequency σ, the cutoff wavenumber $\bar{k}_r$ decreases with a scaling proportional to $Ek^{-1/3}$. Furthermore, for the same value of Ek, the cutoff wavenumber $\bar{k}_r$ also tends to zero as the $\sigma \to 0$ and $\sigma \to 2$, where the focusing effect vanishes. It is easy to understand that the focusing phenomenon disappears when σ tends to 0, because in this case the waves propagate in vertical direction along the cylindrical surface on which the oscillating torus is located according to Eq. (14) and thus do not focus on the z-axis. However, the disappearance of wave focusing at $\sigma \to 2$ is limited to the case where the external force is present only in the z direction. Furthermore, $\sigma \to 2$ corresponds also to the case with an infinitely large viscous effect as described in (37c), so that the energy is rapidly dissipated during propagation and cannot be focused effectively. This prediction remains to be verified by experiments and numerical simulations.

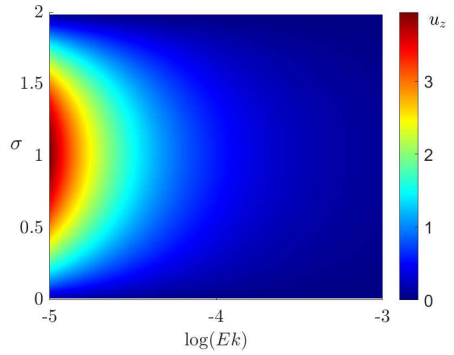

FIG. 6. Amplitude of the vertical velocity at the focal point in a viscous fluid with a slight lowering compared its position in an inviscid fluid ($r = 0$, $z = 1/\alpha$) as a function of the dimensionless frequency σ from 0 to 2 and the Ekman number Ek from 10^{-5} to 10^{-3}.

B. Maximum amplification

Returning to the analytical solution, this allows further properties of inertial wave focusing be analyzed. For example, Fig. 6 shows the change of the amplitude of the vertical velocity at the focal point with the Ekman numbers Ek and the dimensionless forcing frequency σ. For $\sigma \to 2$ and $\sigma \to 0$, corresponding to $\theta \to 0$ and $\theta \to 90°$, respectively, the focusing effect tends to vanish, and its maximum value appears for $\sigma \to 1$, where the oscillating frequency of the torus is close to the angular velocity of the rotating fluid, corresponding to a resonance excitation with an angle of 60 degrees. A similar property has been mentioned by Shmakova and Flór in their investigation[11] for internal waves, but not yet in any study of inertial waves. Furthermore, as the value of the Ekman number increases, the wave beams are no longer straight, but severely distorted near the intersection point, as shown in Fig. 4. In order to understand more precisely the distribution of velocities in the focal zone, we plotted the real part, the imaginary part and the envelope of the wave in (32) along the z-axis for $\sigma = 1$ and the Ekman numbers $Ek = 10^{-5}$, 10^{-4} and 10^{-3}, respectively, see Fig. 7. It shows that with increasing value of Ek, the phase shift increases and accordingly the wavelength becomes longer as well. This phenomenon can be well explained by Eq. (37b), which denotes the phase shift of the waves. For the same σ, the phase shift ψ increases as the Ekman number Ek increases, and the corresponding wave beam becomes wider. At the same time, the position of the wave packet maximum shifts in the negative direction of the z-axis and the wave packet becomes obviously asymmetric. The shift of the peak affected by viscosity compared with the case in the inviscid fluid is also noted in Fig. 7 as the distance between the green line and the black line. The asymmetry is mainly caused by the term $e^{-|z|\alpha\beta k_r^3}$ in the simplified solution in (35). The peaks of the real and imaginary parts of the wave at the focal zone are symmetrically located on both sides of the focal point, but have different amplitudes due to the attenuation factor $e^{-|z|\alpha\beta k_r^3}$. Mathematically, the smaller the $|z|$-value at the crest of the wave beam, the larger the corresponding amplitude. The final position of the maximum after superposition of the two wave beams is biased towards the peak with higher amplitude thus making the envelope asymmetric. Physically we can interpret this phenomenon as an asymmetric distribution of effective viscosity on both sides of the focal point.

In addition, the analytical solution (32) describes also a multitude of structural details of the wave beam. For example, Fig. 8 shows the structure of the wave beam along the radial direction with different values of z before and after wave focusing, respectively. As the wave packet moves away from the torus, the amplitude of the vertical velocity along the direction of the energy propagation first decreases due to viscous attenuation, and then increases due to focusing. After focusing, as the wave moves away from the focal point, the energy of the wave decreases monotonically again due to viscosity. This result is consistent with the study by Ermanyuk *et al.*[22] for internal waves.

IV. CONCLUSIONS

In this work, we have developed a linear analysis of the focusing of inertial waves due to a uniformly rotating fluid. The force exerted by the torus on the fluid particles is considered as an annular line force using Dirac function. The analytical solutions of the velocity field are obtained based on the linear theory for both the inviscid and viscous cases, respectively. The results show that under an axisymmetric forcing, the wave rays form a double cone symmetric about the torus with two focal points, where the wave amplitude has a maximum due to wave focusing. This phenomenon is in good agreement with the experimental and numerical study by Duran-Matute[21]. However, a quantitative comparison with previous experimental and numerical results is still not possible due to the idealization of the model, i.e. neglecting the wave reflection at the container boundary and simplifying the three dimensional structure of the torus. We have also investigated the effect of viscous spreading on the focusing of inertial waves. Our analysis shows that as the Ekman number increases, the wave beam becomes wider, the focusing effect becomes weaker, and the location of the maximal velocity amplitude shifts towards the torus compared with the case in inviscid fluid. Moreover, for the same Ekman number, the focusing effect tends to disappear when the dimensionless oscillation frequency σ is close to 0 and 2, and it is maximal for σ close to 1. This conclusion was not mentioned in the study of Duran-Matute *et al.* and we expect its verification by experiments. Based on the results obtained in this work, we will further analyze the focusing of inertial waves in weakly nonlinear regime and finally explore the localized generation of turbulence around the focal point.

Accepted to Phys. Fluids 10.1063/5.0099774

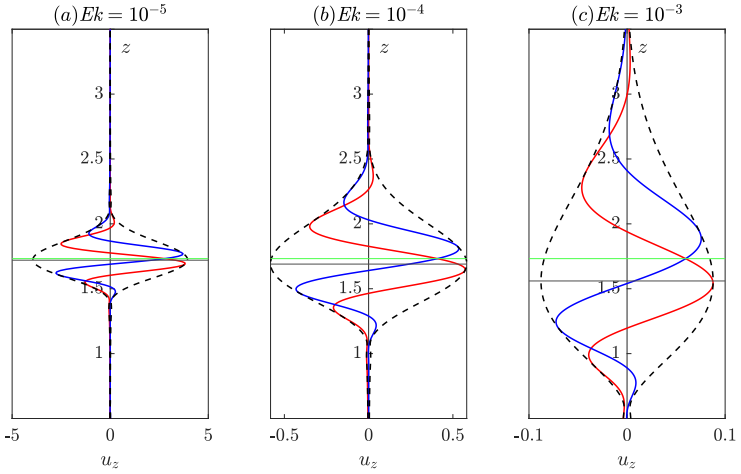

FIG. 7. Envelope (- - -), real part (——) and the imaginary part (——) of the vertical velocity along the z-axis for $\sigma = 1$ in a viscous fluid with the Ekman number (*a*) $Ek = 10^{-5}$, (*b*) $Ek = 10^{-4}$ and (*c*) $Ek = 10^{-3}$, respectively. The green line represents the position of the focal point in an inviscid fluid while the black line shows the lowering of the position of the focal point due to viscosity.

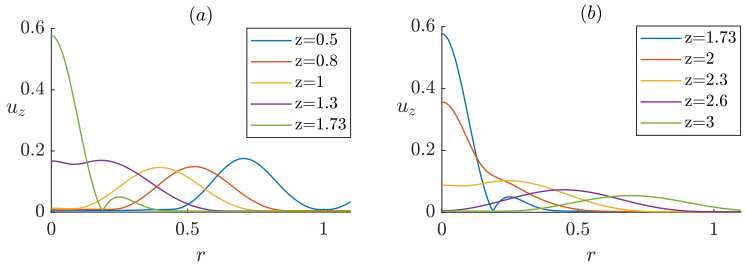

FIG. 8. Structure of the wave beam along the radial direction at different values of z before the wave focusing in (*a*) and after wave focusing in (*b*) with $\sigma = 1$ and $Ek = 10^{-4}$. The focus point is at $z \approx 1.73$.

ACKNOWLEDGMENTS

This work was developed from a German-French joint project and funded by the German Research Foundation (DFG) with Project No. 407316090 and by the Agence Nationale de la Recherche (ANR, French National Research Agency) with Project No. ANR-18-CE92-0034. The authors acknowledge A. Mohamed for fruitful discussions.

Appendix A: Velocity components in the inviscid case

We write the solution of pressure p in (20) for $|\sigma| < 2$ and the forcing $\boldsymbol{f}$ in (8) in the forms

$$p(\boldsymbol{x},t) = P(\boldsymbol{x})e^{-i\sigma t}, \qquad \boldsymbol{f} = \boldsymbol{F}(\boldsymbol{x})e^{-i\sigma t}, \tag{A1}$$

with

$$P(\boldsymbol{x}) = \text{sign}(z) \sum_{m=-\infty}^{+\infty} \frac{\Lambda_m}{2} e^{im\varphi} \times \int_0^\infty k_r J_m(k_r) J_m(r k_r) e^{i\alpha|z|k_r}\, dk_r, \tag{A2}$$

and

$$F_r = 0, \quad F_\varphi = 0, \quad F_z = \sum_{m=-\infty}^{+\infty} \Lambda_m e^{im\varphi}\delta(r-1)\delta(z). \tag{A3}$$

Corresponding to this, the velocity $\boldsymbol{u}$ takes the form

$$\boldsymbol{u}(\boldsymbol{x},t) = \boldsymbol{U}(\boldsymbol{x})e^{-i\sigma t}. \tag{A4}$$

Accepted to Phys. Fluids 10.1063/5.0099774

The Navier-Stokes equation (3) can be projected onto the three directions in cylindrical coordinates

$$-i\sigma U_r - 2U_\varphi = -\frac{\partial P}{\partial r}, \tag{A5a}$$

$$-i\sigma U_\varphi + 2U_r = -\frac{\partial P}{\partial \varphi}, \tag{A5b}$$

$$-i\sigma U_z = -\frac{\partial P}{\partial z} + F_z. \tag{A5c}$$

We can readily manipulate the three equations to express the velocity components in terms of the pressure P and the vertical forcing F_z as following

$$\begin{aligned} U_r =& \frac{1}{4-\sigma^2}\left(i\sigma\frac{\partial P}{\partial r} - \frac{2}{r}\frac{\partial P}{\partial \varphi}\right) \\ =& \text{sign}(z)\frac{i\alpha^2}{2\sigma^2}\sum_{m=-\infty}^{+\infty}\Lambda_m e^{im\varphi}\int_0^\infty e^{i\alpha|z|k_r}\,k_r^2 J_m(k_r) \\ &\times\left[\left(\frac{\sigma}{2}-1\right)J_{m-1}(rk_r) - \left(\frac{\sigma}{2}+1\right)J_{m+1}(rk_r)\right]dk_r, \end{aligned} \tag{A6}$$

$$\begin{aligned} U_\varphi =& \frac{1}{4-\sigma^2}\left(\frac{i\sigma}{r}\frac{\partial P}{\partial \varphi} + 2\frac{\partial P}{\partial r}\right) \\ =& \text{sign}(z)\frac{\alpha^2}{2\sigma}\sum_{m=-\infty}^{+\infty}\Lambda_m e^{im\varphi}\int_0^\infty e^{i\alpha|z|k_r}\,k_r^2 J_m(k_r) \\ &\times\left[\left(\frac{1}{\sigma}-\frac{1}{2}\right)J_{m-1}(rk_r) - \left(\frac{1}{\sigma}+\frac{1}{2}\right)J_{m+1}(rk_r)\right]dk_r, \end{aligned} \tag{A7}$$

$$\begin{aligned} U_z =& -\frac{i}{\sigma}\frac{\partial P}{\partial z} + \frac{i}{\sigma}F_z \\ =& \frac{\alpha}{2\sigma}\sum_{m=-\infty}^{+\infty}\Lambda_m e^{im\varphi}\int_0^\infty k_r^2 J_m(k_r)J_m(k_r r)e^{i|z|\alpha k_r}\,dk_r, \end{aligned} \tag{A8}$$

where $\alpha = \sqrt{\frac{\sigma^2}{4-\sigma^2}}$.

Appendix B: Vertical velocity in the viscous case

According to the solution in Eq. (31) for $\hat{u}_z$ in Fourier space and the inverse Fourier transform defined in Eq. (16), the solution for u_z in the physical space is given as

$$\begin{aligned} u_z =& \frac{i\Lambda_0}{2\pi}e^{-i\sigma t}\int_0^\infty k_r^3 J_0(k_r)J_0(rk_r) \\ &\times\int_{-\infty}^\infty \frac{\sigma + iEk\,k^2}{\left(\sigma + iEk\,k^2\right)^2 k^2 - 4k_z^2}e^{ik_z z}dk_z dk_r. \end{aligned} \tag{B1}$$

If we directly replace k^2 with $k_r^2 + k_z^2$, there are six singularities to consider when using the residue theorem to calculate the integral with respect to k_z. By additional considering the dispersion relation (12), i.e. $\sigma^2 k^2 - 4k_z^2 = 0$, k^2 contained in all viscous terms can be replaced with $\frac{4k_r^2}{4-\sigma^2}$ and then the integral with respect to k_z can be further rewritten as

$$\begin{aligned} I_{k_z} =& \int_{-\infty}^\infty \frac{\sigma + iEk\,k^2}{\left(\sigma + iEk\,k^2\right)^2 k^2 - 4k_z^2}e^{izk_z}dk_z \\ =& -\frac{\sigma(4-\sigma^2) + i4Ek\,k_r^2}{(4-\sigma^2)^2} \\ &\times\int_{-\infty}^\infty \frac{e^{i|z|k_z}}{k_z^2 - \frac{\sigma^2}{4-\sigma^2}k_r^2\left[1 - \frac{64Ek^2k_r^4}{\sigma^2(4-\sigma^2)^3} + i\frac{32Ek\,k_r^2}{\sigma(4-\sigma^2)^2}\right]}dk_z. \end{aligned} \tag{B2}$$

It is to be noticed that the calculation so far does not require low-Ek approximation. The dispersion relation (12) is the same in viscous and inviscid fluid. In the complex k_z-plane, the denominator of the integrand has now only two singularities, which are

$$k_{z1,2} = \pm\alpha(f_1 + if_2) \tag{B3}$$

with $\alpha = \frac{\sigma}{\sqrt{4-\sigma^2}}$ and

$$\begin{aligned} f_1 =& \frac{k_r}{\sqrt{2}}\left\{\sqrt{\left[1 - \frac{64Ek^2k_r^4}{\sigma^2(4-\sigma^2)^3}\right]^2 + \frac{1024Ek^2k_r^4}{\sigma^2(4-\sigma^2)^4}}\right. \\ &\left. + \left[1 - \frac{64Ek^2k_r^4}{\sigma^2(4-\sigma^2)^3}\right]\right\}^{1/2}, \end{aligned} \tag{B4a}$$

$$\begin{aligned} f_2 =& \frac{k_r}{\sqrt{2}}\left\{\sqrt{\left[1 - \frac{64Ek^2k_r^4}{\sigma^2(4-\sigma^2)^3}\right]^2 + \frac{1024Ek^2k_r^4}{\sigma^2(4-\sigma^2)^4}}\right. \\ &\left. - \left[1 - \frac{64Ek^2k_r^4}{\sigma^2(4-\sigma^2)^3}\right]\right\}^{1/2}. \end{aligned} \tag{B4b}$$

Applying the residue theorem[30] (chapter 11.7), the integral (B2) results in

$$\begin{aligned} I_{k_z} =& -\frac{\sigma(4-\sigma^2) + i4Ek\,k_r^2}{(4-\sigma^2)^2}\cdot i\pi\frac{e^{i|z|\alpha f_1}e^{-|z|\alpha f_2}}{\alpha(f_1 + if_2)} \\ =& -i\pi\frac{[\sigma(4-\sigma^2)f_1 + 4Ek\,k_r^2 f_2] + i[4Ek\,k_r^2 f_1 - \sigma(4-\sigma^2)f_2]}{\sigma(4-\sigma^2)^{3/2}(f_1^2 + f_2^2)} \\ &\times e^{i|z|\alpha f_1}e^{-|z|\alpha f_2}. \end{aligned} \tag{B5}$$

[1] H. P. Greenspan, *The theory of rotating fluids* (Cambridge University Press, 1968).
[2] F. Gao, J. W. Chew, and O. Marxen, "Inertial waves in turbine rim seal flows," Phys. Rev. Fluids **5**, 024802 (2020).
[3] K. Aldridge and L. Lumb, "Inertial waves identified in the earth's fluid outer core," Nature **325**, 421–423 (1987).
[4] J. Pedlosky, *Geophysical Fluid Dynamics* (Springer, New York, 1987).
[5] J. Lighthill, *Waves in fluid* (Cambridge University Press, 1978).
[6] P. A. Davidson, *Turbulence in rotating, statified and electrically conducting fuids* (Cambridge University Press, 2013).
[7] I. N. Sibgatullin and E. V. Ermanyuk, "Internal and inertial wave attractors: a review." Journal of Applied Mechanics and Technical Physics **60**, 284–302 (2019).
[8] K. S. Peat, "Internal and inertial waves in a viscous rotating statified fluid," Appl. Sci. Re. **33**, 481–499 (1977).

Accepted to Phys. Fluids 10.1063/5.0099774

[9]N. H. Thomas and T. N. Stevenson, "A similarity solution for viscous internal waves." J. Fluid Mech. **54**, 495–506 (1972).
[10]M. Brunet, T. Dauxois, and P.-P. Cortet, "Linear and nonlinear regimes of an inertial wave attractor." Phys. Rev. Fluids **4**, 034801 (2019).
[11]N. D. Shmakova and J.-B. Flór, "Nonlinear aspects of focusing internal waves." J. Fluid Mech. **862**, R4 (2019).
[12]O. Bühler and C. J. Muller, "Instability and focusing of internal tides in the deep ocean," J. Fluid Mech. **588**, 1–28 (2007).
[13]J. C. Appleby and D. G. Crighton, "Internal gravity waves generated by oscillations of a sphere," J. Fluid Mech. **183**, 439–450 (1987).
[14]S. T. Simakov, "Initial and boundary value problems of internal gravity waves." J. Fluid Mech. **248**, 55–65 (1993).
[15]S. T. Simakov, "Formation of singularities of limiting amplitude in a density stratified fluid disturbed by an extended monochromatic forcing." Wave Motion **19**, 11–27 (1994).
[16]A. Tilgner, "Oscillatory shear layers in source driven flows in an unbounded rotating fluid." J. Fluid Mech. **12**, 1101–1111 (2000).
[17]R. N. Bardakov, A. Y. Vasil'ev, and Y. D. Chashechkin, "Calculation and measurement of conical beams of three-dimensional periodic internal waves excited by a vertically oscillating piston," Fluid Dyn. **42**, 612–626 (2007).
[18]N. Grisouard and O. Bühler, "Forcing of oceanic mean flows by dissipating internal tides." J. Fluid Mech. **708**, 250–278 (2012).
[19]S. Le Dizès, "Wave field and zonal flow of a librating disk." J. Fluid Mech. **782**, 178–208 (2015).
[20]S. Le Dizès and L. Bars, "Internal shear layers from librating objects." J. Fluid Mech. **826**, 653–675 (2017).
[21]M. Duran-Matute, J.-B. Flór, F. S. Godeferd, and C. Jause-Labert, "Turbulence and columnar vortex formation through inertial-wave focusing," Phys. Rev. E **87**, 041001(R) (2013).
[22]E. V. Ermanyuk, N. D. Shmakova, and J.-B. Flór, "Internal wave focusing by a horizontally oscillating torus." J. Fluid Mech. **813**, 695–715 (2017).
[23]N. Shmakova, B. Voisin, J. Sommeria, and J.-B. Flór, "Internal and inertia-gravity wave focusing at large stokes numbers," Phys. Rev. Fluids **6**, 114804 (2021).
[24]B. Voisin, "Internal wave focusing by annular forcing," 8th International Symposium on Stratified Flows, Aug 2016, San Diego, United States (2016).
[25]J. M. Lopez and F. Marques, "Instabilities and inertial waves generated in a librating cylinder," J. Fluid Mech. **687**, 171–193 (2011).
[26]J. M. Lopez and F. Marques, "Rapidly rotating precessing cylinder flows: forced triadic resonances," J. Fluid Mech. **839**, 239–270 (2018).
[27]A. Giesecke, T. Vogt, T. Gundrum, and F. Stefani, "Nonlinear large scale flow in a precessing cylinder and its ability to drive dynamo action," Phys. Rev. Lett. **120**, 024502 (2018).
[28]F. Pizzi, A. Gieseke, J. Šimkanin, and F. Stefani, "Prograde and retrograde precession of a fluid-filled cylinder." New J. Phys. **23**, 123016 (2021).
[29]N. Machicoane, P.-P. Cortet, B. Voisin, and F. Moisy, "Influence of the multipole order of the source on the decay of an inertial wave beam in a rotating fluid," Phy. of Fluids **27**, 066602 (2015).
[30]G. B. Arfken, H. J. Weber, and F. E. Harris, *Mathematical Methods for Physicists: A Comprehensive Guide, 7th Edition* (Academic Press, 2011).
[31]F. Oberhettinger, *Tabellen zur Fourier Transformatioon* (Springer, 1957) pp. 112, 113.
[32]G. K. Batchelor, *An Introduction to Fluid Dynamics* (University of Cambridge, 2000).
[33]P.-P. Cortet, C. Lamriben, and F. Moisy, "Viscous spreading of an inertial wave beam in a rotating fluid," Phys. of Fluid **22**, 086603 (2010).

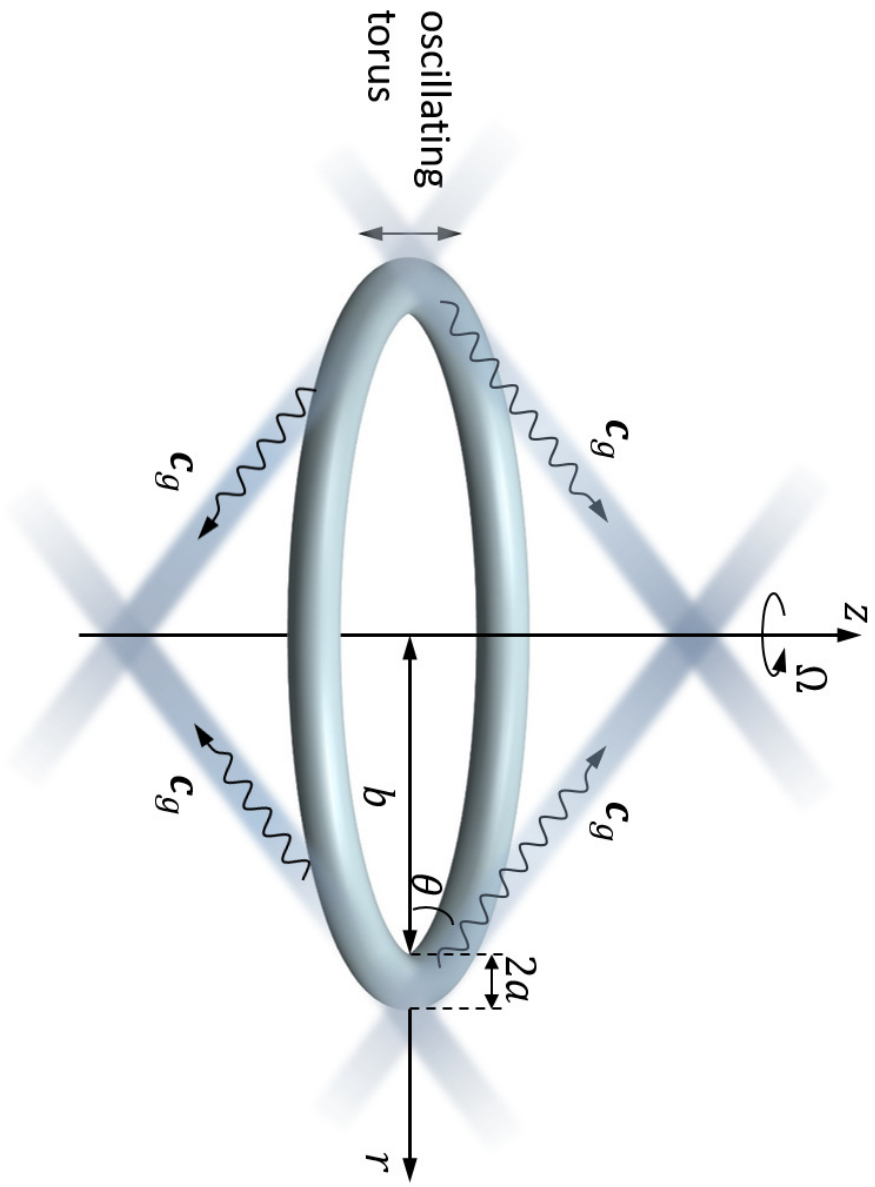

PLEASE CITE THIS ARTICLE AS DOI: 10.1063/5.0099774